strain and temperature, depends on the method of rubbing. The third group includes effects of surface contamination. The last group includes factors inherent in the process of rubbing. Unlike groups two and three, these factors operate, however carefully or cunningly the rubbing be conducted. Thus it comes about that the charges produced by *friction* are not simply those set up by mere *contact*, as in the volta effect.

This paper is experimental. Working on pure elements and the simple refractory material, silica, with improved apparatus and methods, the relation is examined between the volta effect and the triboelectric effect. The two effects prove to be somewhat similar, but there are disparities. The conclusion reached is that, of the four groups in the equation the first is, at least in the case of these specially chosen and carefully prepared materials, paramount for most elements, but not for all.

An X-Ray Investigation of Normal Paraffins near their Melting Points.

By Alex Müller.

(Communicated by Sir William Bragg, F.R.S.—Received July 12, 1932.)

[Plate 13]

Introduction.

The present paper is a continuation of previous work* on the thermal expansion of normal paraffins. It is confined to an investigation of the lattice changes which take place in the range between room temperature and the individual melting points. The observations are rather complex and certain difficulties in the interpretation of the X-ray photographs arise which make further investigations necessary. Such work is now in progress. There were, however, several unexplained points in the last paper which are now clear and dealt with in the present work.

Range of Materials.

The investigation was carried out with 15 specimens ranging from $C_{18}H_{38}$ to $C_{44}H_{90}$. The method of their preparation has been described previously.

* 'Proc. Roy. Soc.,' A, vol. 127, p. 417 (1930).

Experimental.

The problem of the present research was to measure the lattice dimensions at any given temperature between 20° C. (room temperature) and the melting point of the individual substance, the highest being about 90° C. The recording of the lattice dimensions was obtained with the aid of X-ray photographs. It was essential to keep the temperature of the substance constant to a fraction of a degree during the exposure to the X-rays, and it was also desirable occasionally to vary the temperature in small steps of a few tenths of a degree.

The investigation of one single specimen involved sometimes 10 to 20 temperature steps. It was therefore desirable to reduce the time for the temperature adjustment as much as possible. The small thermostat in which the substance had to be kept during the X-ray exposure was heated to the required temperature by a constant flow of preheated water. The water was heated in a small copper tube boiler with a gas burner. There were two ways of adjusting the temperature; one consisted in regulating the gas flame, the other in varying the flow of water. There were three thermometers in the circuit. The first was between the boiler and the thermostat, the second in the thermostat and the third at the outlet. With this arrangement it was possible to estimate the maximum temperature drop in the thermostat itself. This drop did not exceed 1° at the highest temperature recorded and the actual readings were taken at the thermostat thermometer. There were three sets of these used with overlapping scales and each reading to 1/10°.

The thermostat itself was made from a solid copper rod. It weighed about 1 kilogram. It had hollow spaces through which the water circulated and slots through which the incident and the reflected X-ray beams entered and emerged. These slots were either covered with thin nickel foil or cellophane, which stopped any air circulation. The specimen itself, spread on a flat surface at the end of a copper rod, was in the centre of the thermostat. This rod was tapered and fitted tightly in a corresponding seating in the copper block. The thermometer bulb was completely surrounded by copper and close to the specimen. The whole thermostat was supported by three adjustable screws on the table of an X-ray spectrometer. The flat surface on which the substance was spread went through the axis of rotation of the spectrometer. The layer of substance covered about 1/2 sq. cm. and was about one to two-tenths of a millimetre thick. It was obtained by melting a small quantity of the substance on the flat portion of the copper rod.

The spectrometer table carrying the thermostat was oscillated through

about 5° during the exposure. The flat top of the thermostat had a circular scale and the copper rod had a pointer. This made it possible to set the surface of the layer at any required angle relative to the X-ray beam, and to obtain a certain degree of focussing of the reflected rays for a certain region of the spectrum.

The reflected rays after emerging from the thermostat had to pass through a long narrow slot in a shield behind which was a film drum. This drum was turned through a small angle after each exposure, and in this way a whole series of photographs were recorded on the same film. It was easy to measure the shift of any of the recorded lines relative to a reference line, and this was all that was required for the measurement of the expansion. The geometrically correct focussing was, of course, not obtainable for more than one line, but since the actual reflecting range covered only about 10° the lack of correct focussing was hardly appreciable.

The distance between the focus of the X-ray generator and the specimen was about 8 cm. and usually 5·95 cm. between the axis of the spectrometer and the film. Calibration photographs were sometimes taken at twice this distance. A considerable time saving was obtained by the use of an X-ray generator with a rotating anode. The generator had a copper anode and ran as a rule at about 30 KV. and 120–150 milliamps. The average time of exposure was only a few minutes. The temperature adjustment took not more than 5 minutes. The X-rays were, as a rule, filtered by nickel foil and the wave-length used was 1·539 A.

Results.

There are three types of paraffin crystals known so far :—

(1) The normal form. The chains are packed in a prismatic cell of rectangular cross section. The chains are perpendicular to the base of the cell.
(2) A form of lower symmetry. The cross section is not rectangular and the chains may be tilted relative to the base.
(3) A form which has a rectangular cross section (or at least very nearly rectangular cross section) and chains which are tilted relative to the base. This form has been found by Piper and Malkin.

It is found that $C_{18}H_{38}$, $C_{20}H_{42}$ and $C_{22}H_{46}$, when observed at room temperature, belong to the least symmetrical form. $C_{19}H_{40}$ and $C_{21}H_{44}$ show the normal structure and from $C_{23}H_{48}$ up to $C_{34}H_{70}$ both odd and even numbered substances exist in the normal form provided they have previously been molten.

The third form is, as a rule, only observable when the crystals are obtained directly from a solvent. Exceptions to these rules are observed most frequently with substances above $C_{30}H_{62}$. The exact conditions for the occurrence and the stability range of these crystal forms are a subject for further investigations; their study is outside the scope of this paper.

Previous work on the expansion of normal paraffins has shown that the length of the chain axis depends much less upon the temperature than the length of the two other axes. These observations have been confirmed in the present work. The expansion of the c axis (chain axis) is too small to be measured with the apparatus used in the present work. The investigation is essentially confined to the expansion of the two axes which are in a plane perpendicular to the chain axes, and the discussion of the numerical data will mainly deal with those obtained from the normal form.

The planes which are used in this paper for the determination of the "a" and "b" axis, *i.e.*, the two axes which are perpendicular to the chain axis, are all in a zone which contains this chain axis. The actual planes are: 110, 200, 210, 020 and 310, the first two being by far the strongest. These two spacings are indicated in the diagram fig. 1.

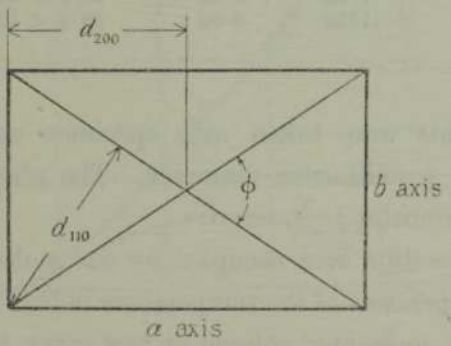

FIG. 1.—Cross section of unit cell (normal form).

The equation connecting the spacings d_{hk0} with the axes and indices is

$$\frac{1}{d^2_{hk0}} = \frac{h^2}{a^2} + \frac{k^2}{b^2}. \qquad (1)$$

There are essentially two unknown quantities which have to be calculated from the observations, namely, "a" and "b"; the indices being known from previous work. Observations were, as a rule, made on the five spacings mentioned above. The method of the least squares was applied in the following form:

$$\Sigma\left(\frac{1}{d^2_{hk0\,(\text{obs.})}} - \frac{h^2}{a^2} - \frac{k^2}{b^2}\right)^2 = \text{minimum}. \qquad (2)$$

The choice of this expression is arbitrary to a certain extent. It has the advantage of making the calculations simple and to give comparatively higher weight to the more accurate observations at large deflecting angles.

The following table gives the result of measurements on a number of paraffins at room temperature. The axes are calculated with the aid of equation (1) and (2) from direct measurements of the five spacings.

Table I.

Number of carbon atoms.	Temperature.	a.	b.	$ab/2$.	ϕ (tan $\phi/2 = b/a$).
	° C.	A.	A.	sq. cm.	° ′
19	19·5	7·55	5·01	$18{\cdot}9 \times 10^{-16}$	67 10
23	18·4	$7{\cdot}43_5$	4·97	$18{\cdot}2 \times 10^{-16}$	67 28
24	18·7	7·41	4·94	$18{\cdot}3 \times 10^{-16}$	67 20
25	18·7	7·41	4·96	$18{\cdot}4 \times 10^{-16}$	67 32
26	19·1	$7{\cdot}41_5$	4·94	$18{\cdot}3 \times 10^{-16}$	67 22
27	19·6	7·40	4·93	$18{\cdot}2 \times 10^{-16}$	67 22
29	19·5	7·42	4·94	$18{\cdot}3 \times 10^{-16}$	67 16
30	19·5	7·33	4·92	$18{\cdot}2 \times 10^{-16}$	67 44
31	19·6	7·40	4·93	$18{\cdot}2 \times 10^{-16}$	67 15
34	19·3	7·40	4·95	$18{\cdot}3 \times 10^{-16}$	67 30
44	20·2	7·33	4·93	$18{\cdot}1 \times 10^{-16}$	67 52

(These measurements were taken with specimen enclosed in thin-walled glass tubes of about $\frac{1}{2}$ millimetre diameter. The glass tubes were centred in the axis of the thermostat.)

$a \,.\, b/2$ is the cross section area occupied by one molecule. Since the chain axis is treated as independent of the temperature in this work, the cross section is proportional to the molecular volume at any given temperature.

The following table shows typical expansion data from a specimen of $C_{23}H_{48}$. The data in this table are calculated from the five observed spacings at each of the given temperatures. The cross section of the specimen at room temperature is taken as a standard. The actual photographs are reproduced on Plate 13. The 110 and the 200 reflection draw closer and closer together and become indistinguishable from each other as the temperature approaches the melting point. The angle ϕ between the diagonals, fig. 1, becomes 60°, showing that the structure changes into hexagonal close packing.

The numerical data of Table II are shown in the following graphs.

The transition from the less symmetrical form into the hexagonal close packing is a continuous function of the temperature.

Table II. $n - C_{23}H_{48}$.

Temperature.	Δa.	Δb.	ϕ.	
°			° ′	
22	±0	±0	66 52	
25	−0·1	0·63	67 10	
30	+2·5	1·2	66 0	a_t observed length of a axis at temperature t.
32	3·4	2·0	65 58	
34	5·3	$1{\cdot}5_6$	64 48	
36	6·4	1·4	64 10	b_t observed length of b axis at temperature t.
37	6·9	$1{\cdot}0_5$	63 48	
38	7·5	0·7	63 20	
45·3	10·9	−1·8	60 0	

$$\Delta a = \frac{a_t - a_{22}}{a_{22}} \cdot 100 \qquad \Delta b = \frac{b_t - b_{22}}{b_{22}} \cdot 100.$$

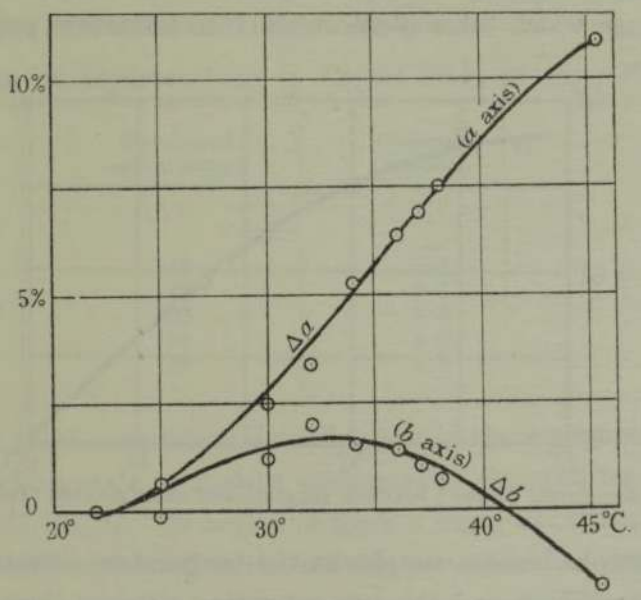

FIG. 2.—Percentage expansion (obs.) of a and b axis (Table II).

$C_{21}H_{44}$ behaves in the same way as $C_{23}H_{48}$. $C_{19}H_{40}$ differs from the two in so far that the substance melts before the symmetrical state is reached, Plate 13. The even numbers C_{18}, C_{20} and C_{22} at room temperature have a different structure compared with the odd numbers. C_{18} and C_{20} do not reach the state of hexagonal packing at the melting point, whereas C_{22} does.

A new phenomenon is observed with $C_{24}H_{50}$. The "a" and "b" axes alter their length as the temperature increases, but this change seems to be much smaller at first. When a certain temperature is reached there is a sudden change in the structure. This is easily seen on the photographs, Plate 13.

The appearance of the photographs alters. Out of the five lines there are only two left, the stronger of the two being only very slightly displaced relative to the 110 line before the transition. The second and weaker of the two shifts into a position about half way between the original 110 and 200 reflection. Occasionally it is found that the original 200 line still persists after the transition, but it is always much fainter than before the transition. Sometimes a number of faint lines are observed. These lines appear to be stronger if a glass tube specimen is used instead of a layer. On one of these photographs as many as six lines are present. All these lines are close to the original 110 and 200 reflection, their spacing being between 3·5 and 4·5 A. The lines with larger reflecting angles seem to vanish. It is only after long exposures—over an hour—and at increased distance, that faint traces of large-angle reflections appear. The existing data are not complete enough to give a picture of the structure change which takes place at the transformation point.

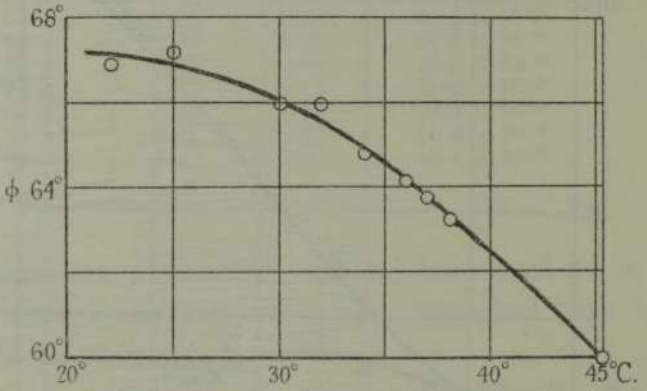

Fig. 3.—Angle ϕ (obs.) between diagonals of cross section (Table II).

The photographs become simpler as the temperature increases. The faint lines vanish very soon and the two remaining stronger lines draw together and behave in the same way as those observed with C_{21} and C_{23}. Near the melting point there is only one line left in the same position as the corresponding lines of C_{21} and C_{23}.

This fact seems to suggest that whatever the structure of the material may be near the transformation point, the final arrangement is again the hexagonal packing. The following table gives the observed spacings corresponding to that single line, which incidentally has already been observed in previous work (*loc. cit.*). The two last columns contain the cross section and also the distance of nearest approach measured between chain axes. The angle ϕ is now 60° for all the specimens in the table.

Table III.—Data on Hydrocarbons in the Solid State near their Melting Point.

Number of carbon atoms.	Melting points.	Observed spacings.	Cross section per molecule.	Distance of nearest approach.
	°	A.	sq. cm.	A.
22	44	4·11	$19·6 \times 10^{-16}$	4·76
23	46	4·17	$20·1 \times 10^{-16}$	4·81
24	51	4·12	$19·6 \times 10^{-16}$	4·76
26	58	4·10	$19·4 \times 10^{-16}$	4·73
27	61	4·06	$19·0 \times 10^{-16}$	4·69
29	64	4·10 4·03 *	$19·2 \times 10^{-16}$	4·68

* Nearly hexagonal.

Photographs of the substances in the molten state show a diffuse band instead of the well-defined lines characteristic of the solid. A few of the observed spacings of molten substances are tabulated below.

Table IV.—Data on Hydrocarbons in Liquid State at their Melting Point.

Number of carbon atoms.	Observed spacing.
	A.
18	4·6
19	4·6
20	4·5
24	4·6
30	4·6

The range of substances which actually go into the hexagonal form seems to be limited. This state of highest symmetry is observed for the numbers 21, 22, 23, 24, 25, 26, 27. 29 begins to show a slight deviation. In C_{30} the two lines are clearly separated at the melting point, and the same holds with the still higher members so far as they have been observed. The same phenomenon is observed with C_{20} and the lower members of the series.

The abrupt transition which occurs with C_{24} is also found for all the higher members. The transition temperature gets closer and closer to the melting point and is almost indistinguishable from it with $C_{44}H_{90}$.

The following table contains the transition temperatures. They were obtained by examining the X-ray photographs taken at different temperatures. No attempt has been made to determine all the transition points very accurately. In the case of C_{26} the temperature steps were narrowed down to fractions of a degree and corresponding X-ray photographs were taken. It was found that the change of the X-ray photograph took place within a few tenths of a degree.

Table V.—Transition temperatures.

Number of carbon atoms.	Transition temperatures between	Melting points.	Difference.
	°	°	°
24	40–41	51·2	10
26	45·5–46	58·0	12
27	48·5–49·3	61	12
29	56·7–57·1	64·4	7
30	58·0–58·3	66·6	9
31	60–64	68·4	6
34	67–68·9	72·8	5
44	85·6–86	86·4	½

These transition temperatures have been measured by Garner* and more recently by Piper† and his collaborators. The present data, for which less accuracy is claimed, agree within the limits of experimental error.

It has been mentioned that the exact interpretation of the X-ray photographs obtained with specimens at the transformation point is not feasible at this stage of development. The large number of lines suggests that the material consists of a mixture of several crystal forms, most of which, however, seem to be stable over only a small range of temperatures. The fact that two of the lines are predominant and behave at higher temperatures like those of C_{21} and C_{23} leaves room for the following speculation.

Assuming that the bulk of the material has essentially the same arrangement as that before the transition has taken place, we may tentatively give the two lines the indices 110 and 200. The new structure differs from the old, in that the axes have different lengths. The data calculated from observations made with C_{29} and C_{24} are :

Table VI.—$C_{29}H_{60}$ Melting Point 63°. Expansion Measurements.

Temperature.	Δa.	Δb.	ϕ.
°			° ′
19·0	±0	±0	67 15
30	0·2	0·4	67 20
40	0·6	$0·6_5$	67 20
51	1·2	0·7	67 0
56·7 trans-	1·6	$0·7_5$	66 50
57·1 formation	6·7	±0	64 20
63	10·5	−0·2	61 20

$$\Delta a = \frac{a_t - a_{19}}{a_{19}} \cdot 100 \qquad \Delta b = \frac{b_t - b_{19}}{b_{19}} \cdot 100.$$

* 'J. Chem. Soc.,' p. 1533 (1931).

† 'Biochem. J.,' vol. 25, pp. 2072–2074 (1931).

The table for C_{29} is arranged identically with that of C_{23}. Up to the transition point the above hypothesis is not involved. The data of this table are plotted in the following graph.

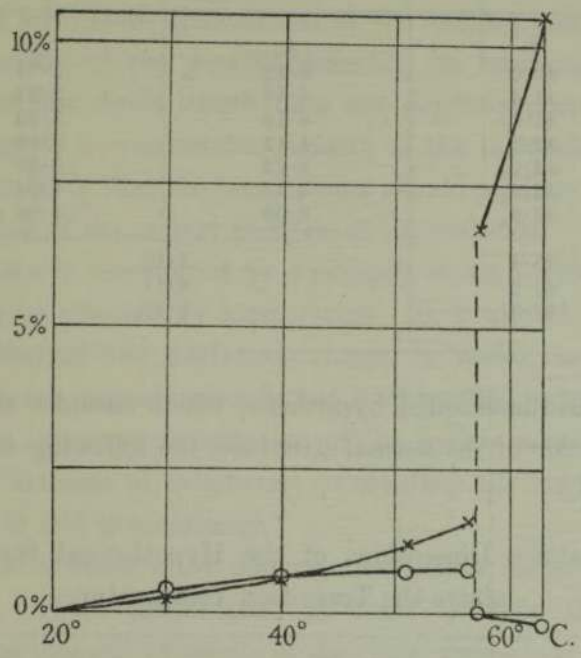

FIG. 4.—Percentage expansion (obs.) of a and b axis (Table VI).

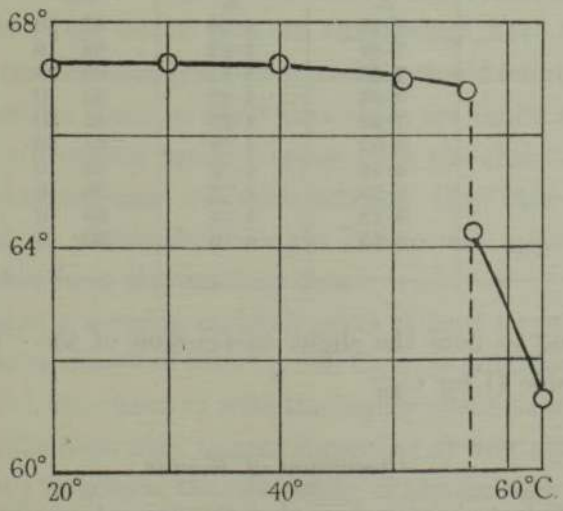

FIG. 5.—Angle ϕ (obs.) between diagonals of cross section (Table VI).

The following table gives the observed spacings of the two strong lines which remain after the substance has gone through the transition.

Table VII.—$C_{24}H_{50}$ Melting point: 51·2° C. Observed Spacings of the two Strong Lines.

Temperature.	d strong.	d weak.
°	A.	A.
40·0	4·12	3·71
41·4_5	4·16	3·91
41·8_7	4·14	3·93
42·5	4·12	3·94
42·9_5	4·12	3·97
43·4_5	4·11	4·01
43·9_2	4·09	4·08
45·4	4·10	
47·9	4·11	
49·3	4·12$_5$	

Using the above-mentioned hypothesis, which assumes that the two lines are the 110 and 200 of the normal structure, the following data are calculated from Table VII.

Table VIII.—Lattice Dimensions of the Hypothetical Structure of $C_{24}H_{50}$ above the Transition Temperature.

Temperature.	a.	b.	ϕ.	$ab/2$.
°	A.	A.	° ′	sq. cm.
Transition 40·0	7·43	4·96	67 26	$18{\cdot}4 \times 10^{-16}$
41·4_5	7·82	4·92	64 16	$19{\cdot}2 \times 10^{-16}$
41·8_7	7·86	4·87	63 34	$19{\cdot}1_5 \times 10^{-16}$
42·5	7·88	4·83	63 0	$19{\cdot}0_5 \times 10^{-16}$
42·9_5	7·95	4·82	62 30	$19{\cdot}1_5 \times 10^{-16}$
43·4_5	8·03	4·79	61 40	$19{\cdot}2_5 \times 10^{-16}$
43·9_2	8·16	4·72	60 0	$19{\cdot}2_5 \times 10^{-16}$
45·4	8·20	4·73	60 0	$19{\cdot}4 \times 10^{-16}$
47·9	8·22	4·74	60 0	$19{\cdot}5 \times 10^{-16}$
49·3	8·25	4·76	60 0	$19{\cdot}6 \times 10^{-16}$

It is interesting to note the slight contraction of the "b" axis, which is also found in Table II for C_{23}.

Discussion of Results.

The data of the last chapter show that the normal paraffins tend to become hexagonal at the melting points. In the range of C_{21} to C_{29} this state of high symmetry is actually reached. Substances outside this range melt before becoming hexagonal.

X-ray investigation has shown that the CH_2 groups in the paraffin molecule are arranged in a zig-zag chain, and that the chains have only two planes of symmetry intersecting in the chain axis. This is found from measurements made at room temperature. The present work shows that the molecules behave as if they were more symmetrical at the melting point.

The inert character of the paraffin molecule, its heat resisting properties and the fact that the chain length does not depend appreciably upon the temperature, suggests a considerable rigidity of the molecular structure. It seems therefore unlikely that the temperature should produce a radical change of the configuration of the carbon skeleton of the molecule.

The carbon chain is surrounded by hydrogen atoms. This hydrogen shell is more likely to be affected by temperature. It is almost certain that the temperature motion of the hydrogens tends to make the molecule more symmetrical at higher temperatures, but it is impossible to tell at the present stage whether the temperature agitation of the hydrogen molecules accounts for the observed increase of symmetry, or whether the zig-zag structure of the carbon chain is still predominant.

The molecule as a whole must perform oscillations under the influence of the temperature. These oscillations also tend to make the crystal more symmetrical. The moment of inertia of the chain molecule is smallest relative to the chain axis. The amplitudes of the oscillations round this axis may become very large at higher temperatures and the molecules may even perform complete rotations. They would then, on the average, have the symmetry of a circular cylinder and the hexagonal close packing would follow quite naturally.

It must, however, be borne in mind that there are limits to the rigidity of the molecule. The frictional forces increase with the chain length and there must be a state when torsional vibration sets in. How this distortion affects the structure, and at which chain length it becomes appreciable, is again impossible to predict from the existing data.

The crude model of a rotating molecule gives at least a qualitative explanation of the phenomena observed with C_{21} and C_{23}. It fails, however, to explain the transitions which are observed with the higher members of the series.

These sudden transitions may appear surprising at first sight. Considering the similarity of the structure, the continuity of the melting points and other physical properties, it does not seem obvious why with two consecutive members of the series, like C_{23} and C_{24}, one should have a transition point and the other not. A qualitative explanation of a similar case has already been given in a previous paper (*loc. cit.*). The argument is this.

The forces which keep the molecules in these crystals together can be divided into two parts. One part of the cohesion can be ascribed to an interaction between the chains, the other between the molecules which form the end groups. These two forces are in equilibrium in the crystal, and the first of the two must depend upon the length of the molecule. The sudden appearance of a transition indicates that the balance of the two forces is sensitive to a small alteration of the chain length at this particular point.

Some of the statements in the last section may be put in a more definite form. Let us consider a chain molecule " A " surrounded by its neighbours. The centres of the circles in the diagram are the intersections of the two rows of carbon atoms in the molecule. The chain axes are in the middle between

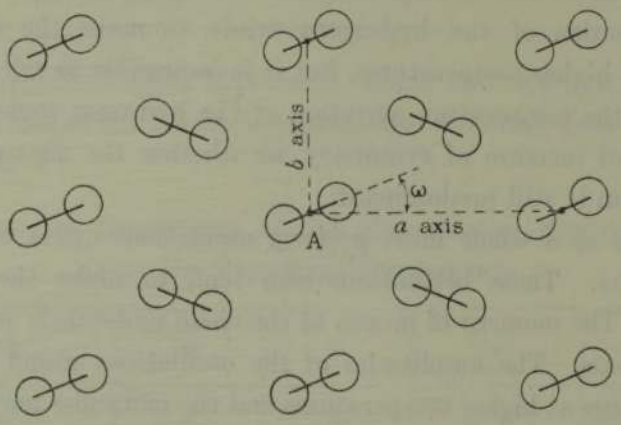

Fig. 6.

the two rows and are perpendicular to the plane of the paper. Let us further assume that the molecule is a rigid body of infinite length. The position of this body is then fixed relative to the crystal lattice by the angle ω. The average position of equilibrium may be called ω_0.

We now introduce the end groups. They are assumed to be so far apart from each other that their interaction is confined to pairs of adjacent layers. It is further assumed that these end groups produce only a small change in the original lattice, and that they are strongly linked to the chains. Supposing the chain forces were eliminated, the end groups would then arrange themselves in their own position of equilibrium—say $\bar{\omega}_0$.

A combination of the two forces is therefore likely to introduce two positions of equilibrium of the chain. The potential energy of the molecule plotted against the angle ω would have a shape as indicated in the diagram. According to the temperature, the molecules would be found more frequently in one or

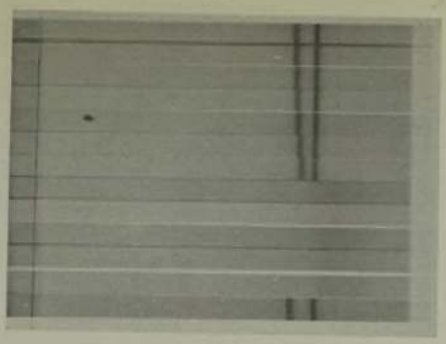

25·1—25·2
26·2—26·2
27·0—27·1
28·0—28·0
29·0—28·9
30·1—30·1
31·1—31·2 n—$C_{19}H_{40}$.
32·1—32·1
32·5—32·7
33·0—33·1
33·6—33·7
33·4—34·1
20·2—19·2

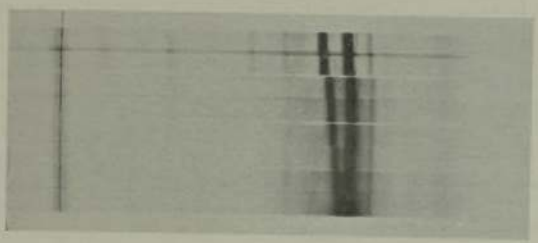

22·05—22·05
25·05—25·05
30·50—29·70
31·95—32·60
34·05—34·60
36·50—35·85
36·90—37·00
37·90—37·95
} n—$C_{23}H_{48}$.
39·7 —39·7
40·0 —40·9
41·9 —41·95
43·0 —43·0
43·95—43·95
45·00—45·00
46·3 —46·2

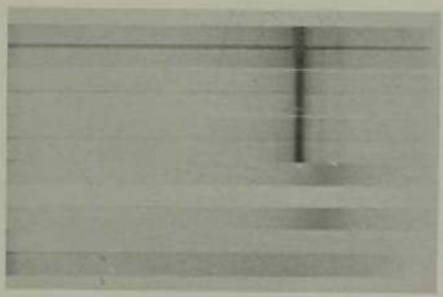

46·95—46·90
47·6 —47·65
19·5 —19·2

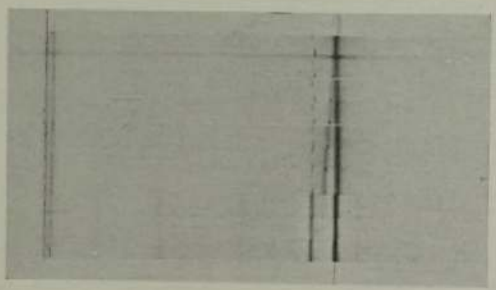

43·90—43·95
43·50—43·40
43·05—42·85
42·55—42·50
41·85—41·80 n—$C_{24}H_{50}$.
41·50—41·40
41·00—40·95
40·05—40·00
38·90—38·75
34·85—

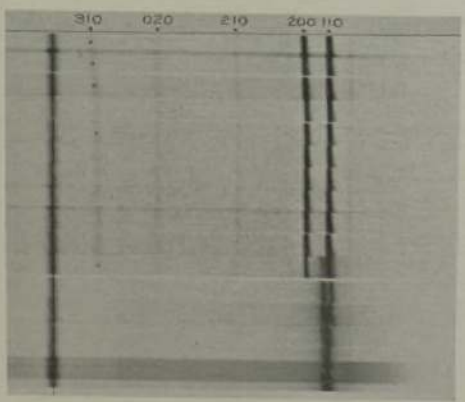

18·45— ·45
30·00— ·10— ·10
39·95— ·80— ·80
48·80— ·80—59·00
51·00—50·75—51·05
51·90—51·95—52·10
53·10—53·00
54·10—54·15 n—$C_{29}H_{60}$.
55·05— ·35— ·05
56·10—55·80—56·05
57·05—56·70—57·00
57·90— ·90
59·90—60·10—59·75
60·95—61·15—60·85
61·95—61·70—61·90
62·85—63·00—63·00

(*Facing p.* 526.)

the other potential valley. This representation, which is not meant to be more than a very crude picture, seems to be the most rational way to account for the observations made in the present work.

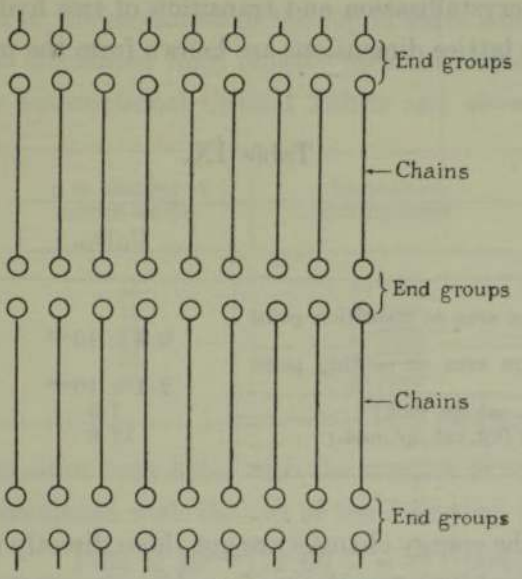

FIG. 7.

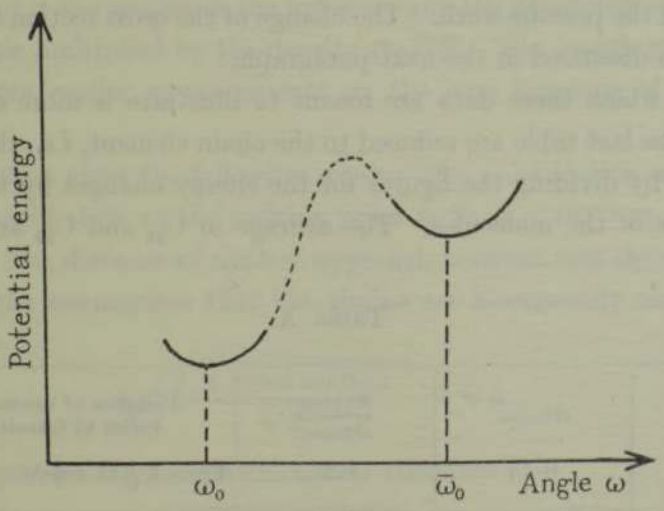

FIG. 8.

Further work is in progress which deals with a more detailed investigation of the disturbing effect of the end-groups, and the effect which is produced when atoms of different kinds are introduced into the chain lattice. It has already been found that oxygen atoms produce a contraction of the carrier lattice. These questions will be dealt with in a separate paper.

In connection with the last section it is of interest to use the data which Garner (*loc. cit.*) has published in his most interesting paper on the heat of crystallisation—and transition of several hydrocarbons. The following table gives the heat of crystallisation and transition of two hydrocarbons for which the changes in the lattice dimensions are known from the present investigation.

Table IX.

	$C_{24}H_{50}$.	$C_{29}H_{70}$.
Change of cross section area at transition point (sq. cm.)	$0{\cdot}8 \times 10^{-16}$	$0{\cdot}7 \times 10^{-16}$
Change of cross section area at melting point (sq. cm.)	$2{\cdot}1 \times 10^{-16}$	$2{\cdot}8 \times 10^{-16}$
Heat of transition (kg. cal./gr. mol.)	7·5	9·8
Heat of crystallisation (kg. cal./gr. mol.)	12·8	15·7

The figures for the energy changes are not those directly measured by Garner but they are obtained by interpolation from his measurements. The change in cross section at the transition points are taken from Tables VI and I and Table VIII of the present work. The change of the cross section at the melting points will be discussed in the next paragraph.

The point which these data are meant to illustrate is more clearly seen if the data of the last table are reduced to the chain element, *i.e.*, the CH_2 group. This is done by dividing the figures for the energy changes by the number of carbon atoms of the molecules. The average of C_{24} and C_{29} are used in the next table.

Table X.

$E_{Trans.}$	$\Delta_{Trans.}$	$\frac{E_{Trans.}}{\Delta_{Trans.}}$	Distance of nearest approach varies at transition point:
0·34	0·75	4·3	From 4·5 to 4·6 A.
E_{Fusion}	Δ_{Fusion}	$\frac{E_{Fusion}}{\Delta_{Fusion}}$	At the melting point:
0·54	2·2	2·2	From 4·7 to 5·0 A.

$E_{Trans.}$ = heat of transition
E_{Fusion} = ,, crystallisation
} in kg. cal./gr. mol. CH_2.

$\Delta_{Trans.}$ = change in cross section p. mol. at transition point
Δ_{Fusion} = ,, ,, ,, melting point
} in 10^{-16} sq. cm.

This table gives an indication of the energy-changes involved at the transition—and melting point. The two ratios show the rapid decrease of the internal energy with increasing distance of the molecules (2·2 against 4·3).

The cross sections of the molecules in the liquid state which are used in the previous section are calculated from density measurements. These densities are taken from the International Critical Tables and show that the density

n = number of carbon atoms.	Density at melting point.
15	0·7761
16	0·7767
17	0·7766
18	0·7770
20	0·7778

at the melting point alters very little with the number of carbon atoms. The cross sections are calculated with the aid of the following expression:

$$\text{Cross section} = \frac{1{\cdot}66 \times 10^{-24}\,(12{\cdot}00 \times n + 1{\cdot}008\,[2n + 2])}{(1{\cdot}253 \times n + 2{\cdot}30) \times 10^{-8} \times 0{\cdot}778}.$$

The numerator is the weight of the molecule and the denominator is the length of the molecule multiplied by the density (0·778). The length of the molecule is derived from earlier measurements on the long spacings of these hydrocarbons.*

The calculation gives the following result: The cross section area of a molecule in the liquid state at the melting point is $22{\cdot}0 \times 10^{-16}$ sq. cm. (average C_{20} to C_{30}). The distance of nearest approach between two chain axes, calculated under the assumption that the chains are hexagonally close packed in the liquid, is

$$\sqrt{\frac{2 \times \text{cross section}}{\sqrt{3}}} \sim 5{\cdot}0\ \text{A.},$$

and the largest spacing in this hexagonal structure:

$$\sqrt{\frac{\text{cross section} \times \sqrt{3}}{2}} \sim 4{\cdot}3\ \text{A.},$$

The observed spacings of the liquid at the melting point are all about 4·6 A. according to Table IV.

* These measurements were made on substances in the solid state. Owing to the negligible expansion of the chain axes and the comparatively small gaps at their ends, the use of these data is not introducing an appreciable error.

We therefore find:

Distance of nearest approach of hexagonally packed chains (calculated from density of liquid)	Observed spacing liquid at melting point	Spacing calculated from density (hexagonally packed chains)
5·0 A.	4·6 A.	4·3 A.

The distance of nearest approach is measured from chain axis to chain axis. The observed X-ray spacing lies about half way between the distance of nearest approach and the spacing calculated from the density of the liquid.

The writer wishes to express his appreciation to Sir William Bragg, O.M., F.R.S., and the Managers of the Royal Institution for their kind interest in the work.

Summary.

(1) The lattice dimensions of a number of hydrocarbons are measured at different temperatures between 20° and the individual melting points.

(2) It is found that $C_{21}H_{44}$, $C_{22}H_{46}$, $C_{23}H_{48}$, $C_{24}H_{50}$, $C_{25}H_{52}$, $C_{26}H_{54}$, $C_{27}H_{56}$ and $C_{29}H_{60}$ change from a state of lower symmetry into hexagonal symmetry. This state is reached when the substances are solid and near the melting point.

(3) The lower members of the series, *i.e.*, C_{18}, C_{19} and C_{20}, and also those above C_{29}, tend to approach hexagonal symmetry, but melt before they reach this state.

(4) C_{21} and C_{23} show a continuous change of the "a" and "b" axes with increasing temperature up to the melting point. C_{24}, C_{25}, C_{26}, C_{27}, C_{29}, C_{30}, C_{31}, C_{34} and C_{44} show abrupt transitions between room temperature and the individual melting points.

(5) Using Garner's data on the heat of crystallisation and transition, and the lattice changes measured in this work, it is found that the lattice energy decreases very rapidly with increasing molecular distance.

(6) Attention is drawn to the fact that paraffins of moderate chain length may be regarded as rigid rotators. Attempts are made to explain the transitions from general principles.